

Cadmium accumulation dynamics in the rice endosperm during grain filling revealed by autoradiography

Atsushi Hirose^{1,2}  | Keitaro Tanoi² | Tomoko M. Nakanishi² | Natsuko I. Kobayashi^{1,2} 

¹Department of Pharmacology, Hoshi University, Tokyo, Japan

²Graduate School of Agricultural and Life Science, The University of Tokyo, Tokyo, Japan

Correspondence

Natsuko I. Kobayashi, Graduate School of Agricultural and Life Science, The University of Tokyo, 1-1-1 Yayoi, Bunkyo-ku, Tokyo 113-8657, Japan.
Email: anikoba@g.ecc.u-tokyo.ac.jp

Funding information

This work was supported by the Japan Society for the Promotion of Science (Grant-in-Aid for Scientific Research (A): 20H00437 and (B): 23H02110) and partially by a grant from the Ministry of Agriculture, Forestry and Fisheries of Japan (Molecular cloning and characterization of agronomically important genes of rice: IPG0009) to TMN.

Abstract

Cadmium (Cd) is one of the environmental pollutants contaminated in our food. Several previous reports showed that rice polishing cannot be efficient to reduce Cd content in white rice, implying the characteristic Cd distribution in rice grain. However, Cd distribution has not been fully elucidated so far. Herein, ¹⁰⁹Cd radiotracer experiment was performed using the rice seedlings at various time points after flowering to obtain autoradiographs of the brown rice to visually understand the Cd transport and distribution during the grain-filling process. It was shown that ¹⁰⁹Cd accumulated in the outermost area of the brown rice, and also in the middle part of the starchy endosperm, resulting in the appearance of the double circle distribution pattern, which was not observed in the autoradiographs of ⁶⁵Zn. The inner circle of ¹⁰⁹Cd located around the center of the endosperm was developed particularly at around 8 and 10 days after flowering. After this period, ¹⁰⁹Cd started to deposit at the outer part of the endosperm, which was also found in the autoradiograph of ¹⁴C-sucrose. Considering the physiology of grain development, the contribution of water transport and protein synthesis in the endosperm on the characteristic Cd distribution pattern was hypothesized.

KEYWORDS

cadmium, endosperm, radiography, rice, tracer, visualization

1 | INTRODUCTION

Cadmium (Cd) is one of the hazardous metals present in food. It comes from soil and water which naturally contain some amount of cadmium. If the amount of Cd in the environment increases and the Cd content of crops increases, it can lead to negative effects on human health. The famous severe chronic Cd poisoning known as itai-itai disease occurred in the mid-19th century in Japan, due to the river water contaminated with slags containing Cd delivered from the mine upstream (Yoshida, 2002). The symptoms of itai-itai disease are renal tubular dysfunction and osteoporosis, which are accompanied by back

pain, muscle pain, and other painful symptoms. Even without concentrations high enough to cause such symptoms, low-level Cd exposure has been noted to be associated with reduced bone mineral content and increased cancer risk (FAO/WHO, 2011b).

To avoid the health damage caused by excess Cd accumulation in the body, provisional tolerable weekly intake (PTWI) for Cd is determined to be 7 mg/kg-body-weight/month by FAO/WHO, and accordingly, the maximum levels for Cd in each food is determined. Given that rice is the staple food in Asian countries, reducing the Cd content in rice grains as low as possible is directly attributable to the achievement of reducing health risks.

This is an open access article under the terms of the [Creative Commons Attribution-NonCommercial](https://creativecommons.org/licenses/by-nc/4.0/) License, which permits use, distribution and reproduction in any medium, provided the original work is properly cited and is not used for commercial purposes.

© 2024 The Authors. *Plant Direct* published by American Society of Plant Biologists and the Society for Experimental Biology and John Wiley & Sons Ltd.

There are several methods to reduce Cd content in rice. Washing the soil to remediate the Cd-contaminated paddy soil is one of those methods. For washing, several reagents such as hydrochloric acid solution (Takijima et al., 1973), ethylenediaminetetraacetic acid (EDTA) solution (Abumaizar & Smith, 1999; Nakashima, 1979), methylglycine diacetate tri-sodium (Makino et al., 2011), and calcium chloride (Makino et al., 2007) were tested and their effects on removing Cd were presented. After starting rice cultivation, keeping the paddy fields flooded is effective to reduce the Cd content in rice grains (Arao et al., 2009; Carrijo et al., 2022). This water management method is based on the chemical property of Cd. Under the reduced condition in flooded soil, the solubility of Cd decreases and it precipitates as carbonate (Khaokaew et al., 2011) and/or as sulfide (de Livera et al., 2011), which the rice root cannot absorb.

Polishing rice grains to obtain white rice before cooking is effective to remove various elements. Therefore, polishing of rice is a general-purpose measure that consumers can do by themselves to reduce contamination by toxic elements. The effectiveness of polishing in reducing the radiocesium contamination in rice has been actively verified in Japan after the nuclear power plant accident in Fukushima. When the polishing ratio (mass ratio of polished rice to brown rice) was 90–92%, which is typical for the rice marketed as white rice, radiocesium concentration in the rice was decreased to almost half of that before polishing (Hachinohe et al., 2015; Tagami & Uchida, 2012). The radiocesium concentration was further decreased to almost 20% as the polishing ratio decreased to 70% (Okuda et al., 2013). Arsenic contamination of rice is an urgent issue in several Asian countries (FAO/WHO, 2011a). The polishing ratio of 90% achieved the total arsenic level decreased to 61–66% of that in brown rice (Naito et al., 2015). Pedron et al. (2019) further demonstrated that polishing rice for 60 seconds using a rice mill Suzuki MT-10 could remove more than 40% of arsenic. On the other hand, the effectiveness of polishing rice as a Cd-mitigation method is less clear. Polishing rice for 60 seconds removed only 17% of Cd (Pedron et al., 2019). According to the report comparing Cd and arsenic concentrations in 48 rice samples, the median Cd concentration in polished rice was 92% of that of unpolished rice while it was 73% for arsenic (Onozuka et al., 2000). It was also shown that the polishing ratio of 96% had mealy effective in reducing Cd concentration, and the Cd concentration in polished rice was still 94% of that of brown rice when the polishing ratio reached 91%. This value of Cd, 94%, was apparently higher than other metals such as manganese (Mn), iron (Fe), and zinc (Zn) which showed 34%, 21%, and 79%, respectively (Shindoh & Yasui, 2003). It will therefore be important to note that the distribution of Cd in brown rice may be very different from those of other metals.

Recently, the distribution of Cd as well as other metals in mature brown rice was imaged using synchrotron-based X-ray absorption spectroscopy (Gu et al., 2020). It was found that Cd can be distributed almost uniformly, or concentrated higher in the outer portions of starchy endosperm and to the aleurone layer, probably depending on the timing of the supply of Cd from the soil (Gu et al., 2020). These distribution patterns were unique to Cd and contrasting to those of Mn,

Fe, and Zn, which accumulated mainly in the embryo and the aleurone/pericarp layer (Gu et al., 2020). The unique Cd distribution in the outer portions of the starchy endosperm was consistent with the Cd distribution profile obtained by laser ablation-inductively coupled plasma-mass spectrometry (Wei et al., 2017). Then, how is this unique Cd distribution pattern developed? Knowledge of this not only contributes to scientifically verifying the effectiveness and limitations of polishing rice as the Cd-mitigation method but also provides important clues to elucidate the molecular mechanisms of Cd accumulation in rice grains. In this study, we addressed this issue by investigating the distribution pattern of Cd, with zinc (Zn) distribution as a comparison, in rice grains through the grain-filling and maturing stages over 28 days. Autoradiography technique using ^{109}Cd visually revealed that the Cd distribution in rice grains dynamically changes with the timing of the input into the grain, and finally, in mature brown rice, a unique “double circle” distribution pattern was developed, consisting of an inner circle due to Cd accumulation in the middle part of the starchy endosperm, and an outer circle due to Cd deposition in the cross cells, the tube-cells, and the seed coat tissue, outside of the aleurone layer.

2 | RESULTS

2.1 | Unique distribution pattern of ^{109}Cd found in the growing brown rice

The transition into the distribution of each inorganic element in mature brown rice was depicted by the sequential visualization of radiotracers, ^{109}Cd and ^{65}Zn , which were dosed to the rice plant continuously from the ear emergence until harvesting. The autoradiographs of ^{109}Cd showed that Cd distributed almost uniformly in the grain at 3 DAF (days after flowering) and 6 DAF. At 9 DAF, ^{109}Cd started to distribute surrounding the center of the grain, at the abaxial side of scutellum, and in the outermost part of the grain (Figure 1a). In the transverse section, ^{109}Cd signal appeared like a double circle (Figure 1a,b). When expressed three-dimensionally, the ^{109}Cd accumulation area in the endosperm was shaped like an elongated balloon connecting to the abaxial side of scutellum. Thereafter, the distribution of ^{109}Cd does not change largely until 28 DAF when the rice grain matured (Figure 1a). Zinc was initially accumulated in the outermost part of the grain and the embryo, but from 9 DAF, it was distributed also in the central area of the endosperm (Figure 1a). As a result, ^{65}Zn signal was detected almost uniformly at 28 DAF, except in the embryo where it was extremely strong (Figure 1b).

Having detected the unique accumulation pattern of Cd, we next tried to see whether the formation of the double circle pattern of Cd distribution in the brown rice, especially the inner circle surrounding the center of the endosperm, was completed around 9 DAF to 12 DAF, or whether Cd entering the endosperm after 9 DAF continued to be deposited there until rice matures. For this purpose, we dosed ^{109}Cd to the rice root for only 24 hours at various points after flowering and traced its distribution in the brown rice after 2, 5, and

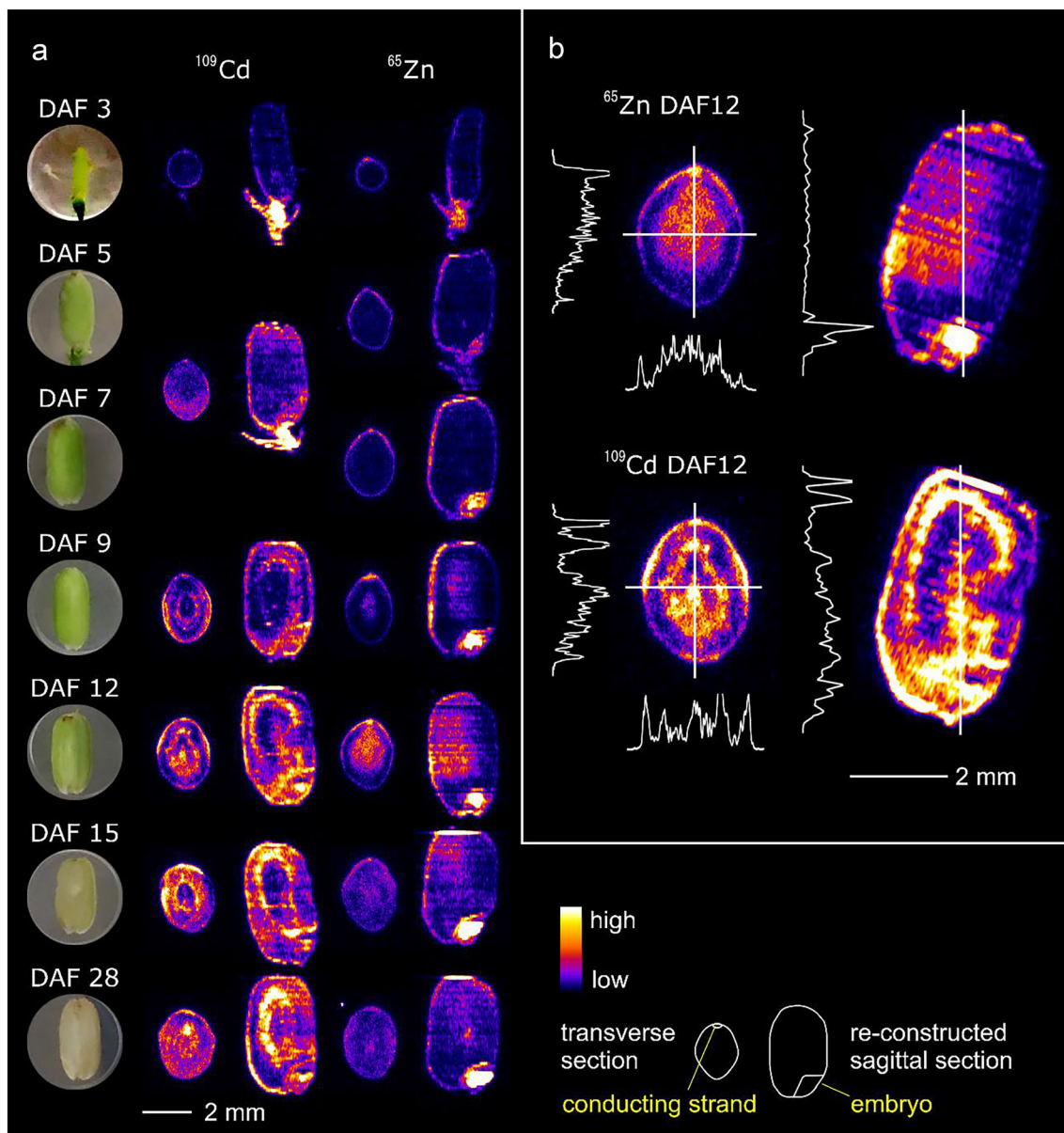


FIGURE 1 Distributions of Cd and Zn in rice grain during the maturation process. (a) The images of ^{109}Cd and ^{65}Zn distribution in the vertical transverse section and the sagittal views are shown. The number of days after flowering (DAF) at the sampling and the appearance of the grain then are presented on the left. (b) Quantification of the intensities of ^{109}Cd and ^{65}Zn signals along the lines in the grain samples harvested 12 days after flowering. The strength of the signal is shown in logarithm.

8 days and at the maturation stage. We refer, for example, to brown rice in which the addition of ^{109}Cd was started on 3 DAF and was sampled for autoradiography 2 days after, that is, 5 DAF, as the 3–5 DAF rice sample.

The distribution of ^{109}Cd in the endosperm of 3–5 DAF samples was almost uniform (Figure 2a). But in the autoradiographs of, 3–8 DAF and 6–8 DAF samples, formation of ^{109}Cd inner circle was started, and the ^{109}Cd signal was clearly observed as double circle in 3–11 DAF and 6–11 DAF samples (Figure 2a–d). On the other hand, the inner circle was less clear in 9–11 DAF sample as well as in 9–14 DAF and 9–17 DAF samples (Figure 2a). Therefore, the development of the inner circle was thought to be started in 8 DAF and was mostly

completed before 11 DAF. The ^{109}Cd distribution observed by 11 DAF commonly had a strong signal near the apical part of the sample, probably corresponding to the dorsal vascular tissues (Figure 2a). In the 9–11 DAF, 9–14 DAF, 9–26 DAF, 12–14, 12–17 DAF, 12–20 DAF, and 12–26 DAF samples, ^{109}Cd did not reach the central part of the endosperm, but was slightly spread from the dorsal vascular tissues to the outer area of the endosperm, with little contribution to the formation of the inner circle (Figure 2a–c). In the rice samples to which ^{109}Cd was added from 15 DAF to 16 DAF, the signal intensity was very low, but it was apparently observed that ^{109}Cd was accumulated preferentially in the outermost part of the brown rice (Figure 2a–c).

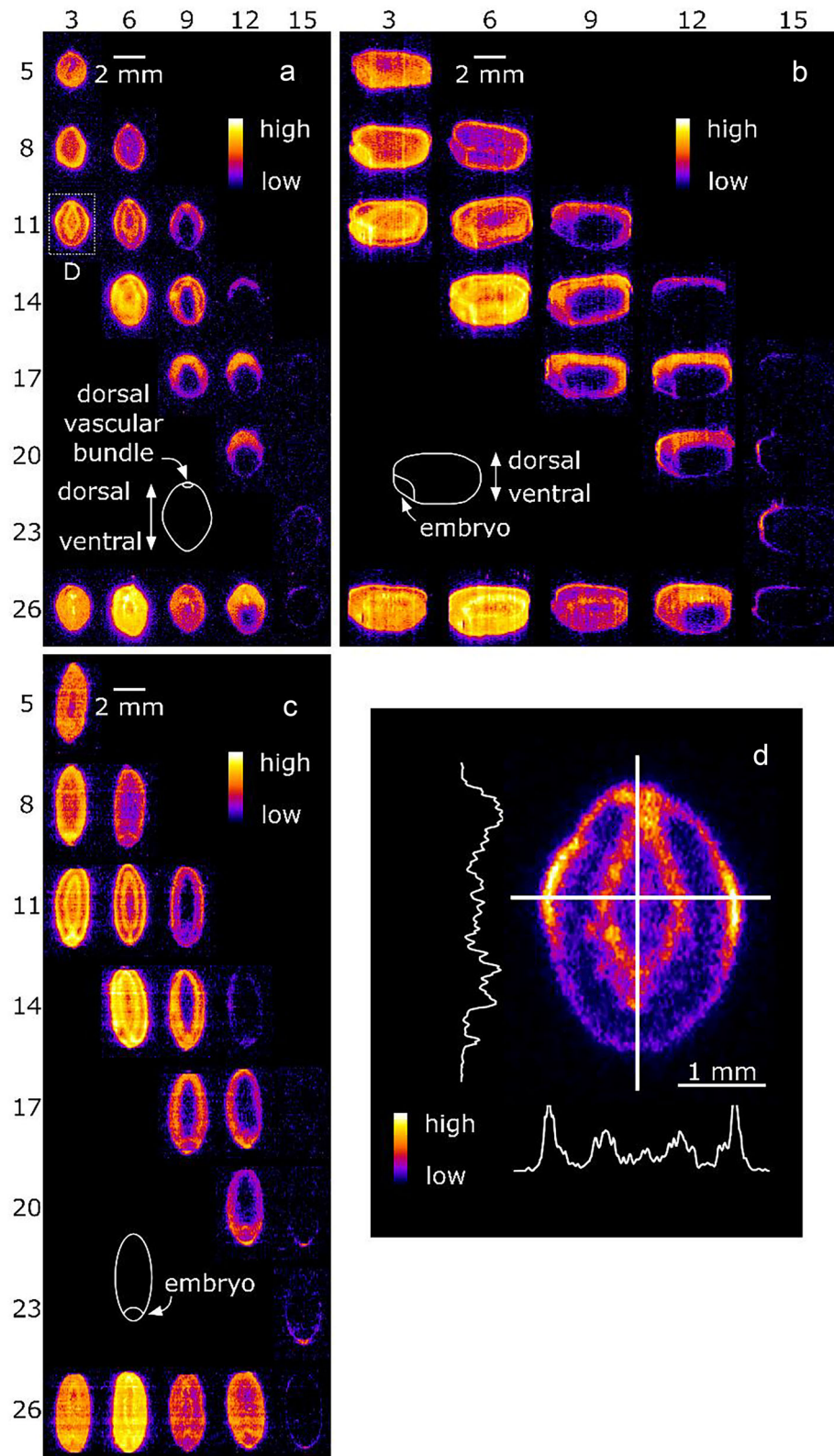


FIGURE 2 Distribution of ^{109}Cd added at multiple time points during the maturation of brown rice. The number of days after flowering (DAF) at the time when the 24 hours of ^{109}Cd absorption was started is indicated on the horizontal axis. The DAF at the time the sample was taken is indicated on the vertical axis. (a) The vertical transverse section images. The sagittal view (b) and the horizontal longitudinal view (c) are created digitally using the reconstructed three-dimensional ^{109}Cd distribution data. (d) The ^{109}Cd signal intensity values along the lines drawn in the 3–11 DAF sample. The strength of the signal is shown in logarithm.

2.2 | High-resolution analysis of ^{109}Cd distributed in the double circle pattern at 11 DAF

Identifying the tissue where exactly Cd accumulated at the time point when the double circle pattern of Cd distribution became the next

challenge. Therefore, the microautoradiography (MAR) method for the fresh-frozen plant section was applied to the 3–11 DAF sample. As a result, inside the endosperm area, it was shown that the ^{109}Cd signals looked as if they were arranged in an oval shape from a distance were not actually aligned in a line, but were scattered discontinuously

around the central portion of the endosperm (Figure 3a). According to the overlaid picture of the ^{109}Cd signal image and the hematoxylin-stained section image, ^{109}Cd appeared to be localized intracellularly rather than in intercellular spaces (Figure 3a). Meanwhile, as far as the hematoxylin-stained images were concerned, there was nothing characteristic about the cells in which ^{109}Cd was localized in the endosperm spaces.

In the outer part of brown rice, ^{109}Cd was accumulated almost on the surface layer (Figure 3a). In contrast to being scattered in the endosperm, ^{109}Cd was distributed continuously on the arc of the ellipse. However, the ^{109}Cd signal varied in intensity depending on the location: the strongest signal was detected around left and right sides of the ellipse, followed by a stronger signal at the apex (Figure 3a). To distinguish which cell type ^{109}Cd localized to, the non-separated MAR method was carried out (Figure 3b). In this method, the fresh-frozen section covered with a layer of the nuclear emulsion was developed to deposit the silver particles directly on the section so that not the slightest positional misalignment would occur during overlaying the ^{109}Cd signal image and the tissue image. Microscopic examination revealed that silver particles were deposited around the tube cells and the cross cells, as well as in the adjacent seed coat tissue consisting of the inner integument and the nucellar epidermis, while few were observed in the aleurone layer adjacent to the inner side of the seed coat (Figure 3b).

2.3 | Comparison of transport patterns of ^{109}Cd and ^{14}C -sucrose

It was assumed that Cd flows into endosperm along with the transport of the photoassimilates. To evaluate this, the distribution of ^{109}Cd at different stages of maturation was compared with that of foliar-applied ^{14}C labeled sucrose. When ^{109}Cd was dosed from 9 DAF and observed 1, 2, 4, and 7 days later, ^{109}Cd was found to be distributed in the outer endosperm, especially in the upper dorsal side (Figure 4a). Then, looking at the ^{14}C signal at the same period, ^{14}C was found to be accumulated in the outer region of the endosperm almost uniformly (Figure 4a). The characteristic of not flowing into the inner region of the endosperm was commonly observed in both radiotracers. In the brown rice to which the radiotracers were administered at 15 DAF, ^{109}Cd as well as ^{14}C signal was detected particularly at the outermost region of the brown rice, and hardly distributed inside the endosperm (Figure 4a). Thus, the similarities and differences between the distributions of the two nuclides were largely understood. However, we could not rule out the possibility of misjudgment on the colocalization of ^{109}Cd and ^{14}C since the layout of the radiotracer can differ to some extent from sample to sample, which is the so-called individual difference. So, in order to make precise comparisons without taking individual differences into account, both ^{109}Cd and ^{14}C -sucrose were administered from 9 DAF to 10 DAF to the same seedling, and their distributions were analyzed in the same

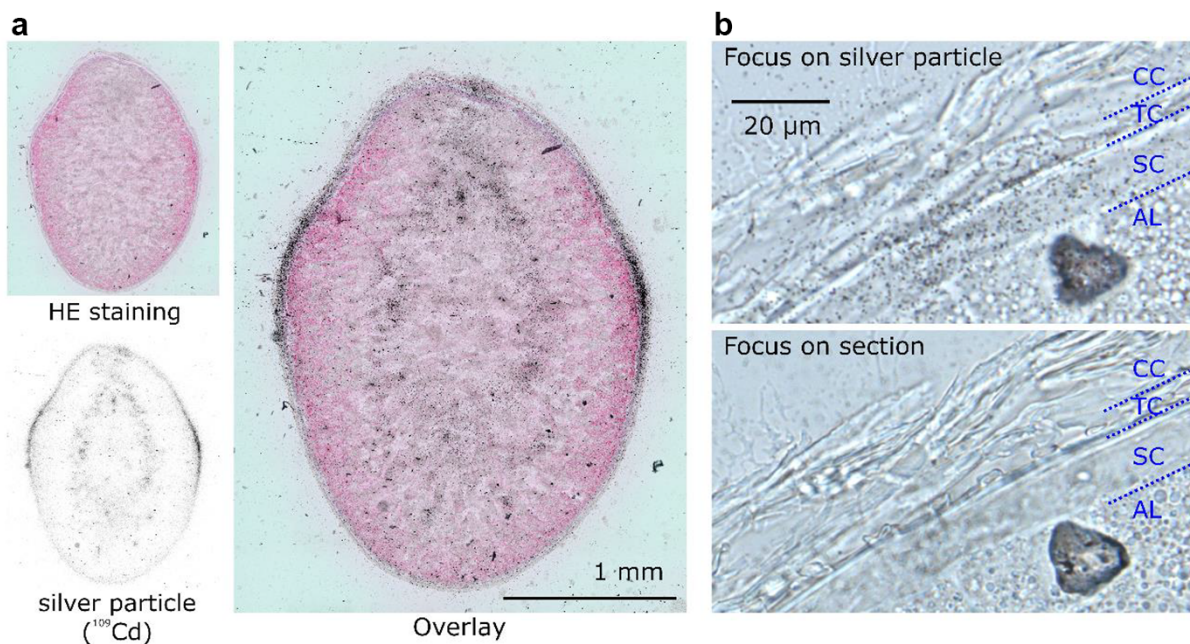


FIGURE 3 Identification of ^{109}Cd localized tissue in the grain sampled at 11 days after flowering (DAF) at high resolution using 2 types of microautoradiography (MAR) methods. (a) Separated MAR method shows the distribution of ^{109}Cd over the entire surface of the vertical transverse section. The section images of hematoxylin–eosin (HE) stained section sample and the images of silver particle corresponding to the radiation energy of ^{109}Cd are overlaid. (b) Non-separated MAR method allows the observation of silver particles developed on the section. The same sample was observed by focusing on the silver particle (upper panel) or the section (lower panel). The images are the observation of the outermost part of brown rice, including the cross cells (CC), the tube cells (TC), the seed coat (SC), and the aleurone layer (AL).

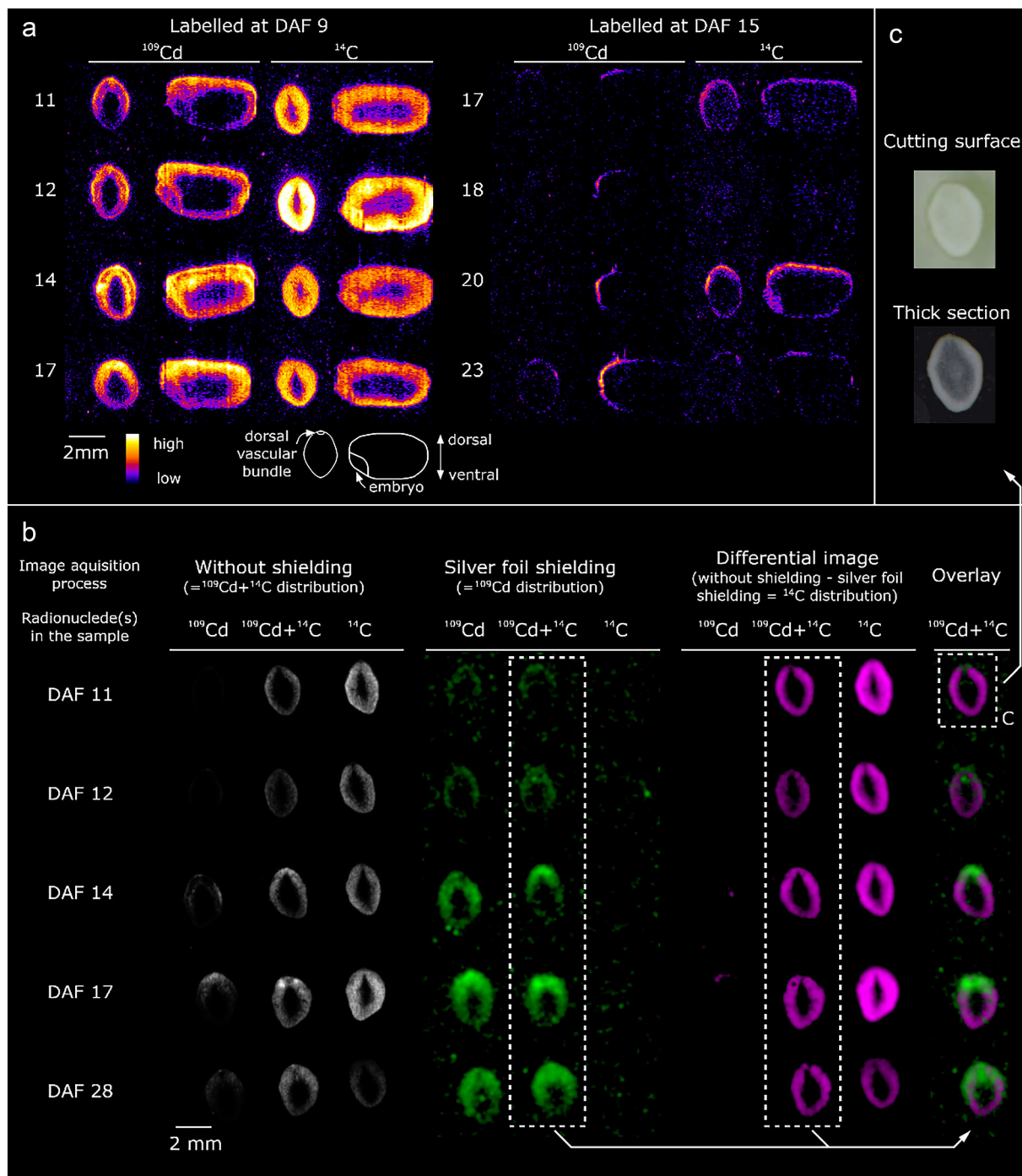


FIGURE 4 Comparison of the distribution patterns of ^{109}Cd and ^{14}C in rice grain. ^{109}Cd was absorbed from roots, and ^{14}C -sucrose was added to the flag leaf surface. (a) ^{109}Cd and ^{14}C -sucrose were introduced to the rice plant for 24 hours from either 9 DAF or 15 DAF, and then visualized at the day (DAF) indicated on the left. (b) ^{109}Cd and ^{14}C -sucrose were introduced simultaneously to the same rice plant from 9 DAF (indicated as “ $^{109}\text{Cd} + ^{14}\text{C}$ ”), and the grains were harvested on the day indicated on the left. For the technical validation, the samples in which ^{109}Cd and ^{14}C -sucrose were absorbed separately were also prepared and visualized (indicated as “ ^{109}Cd ” and “ ^{14}C ”). The silver foil completely shielded the ^{14}C signal, making it possible to discriminate ^{109}Cd and ^{14}C distributions in the same grain sample (see Section 4). (c) The cut surface of the rice sample, and the transmitted light image of the rice section with 1 mm thickness taken at 11 DAF (its radiography is enclosed by a dotted square in b).

brown rice (Figure 4b). One day after, the ^{14}C signal was already distributed in the outer parts of endosperm in contrast to the ^{109}Cd signal which was detected only at the dorsal part of the brown rice.

After that, the location of ^{109}Cd accumulation expanded over the days, but did not quite reach the ventral part of the endosperm until 18 days later (Figure 4b). On the other hand, the region in the inner



parts of endosperm where ^{109}Cd and ^{14}C did not go in was found to be identical for both radiotracers (Figure 4b). This region has already begun to become transparent at 11 DAF (Figure 4c), indicating that carbohydrate filling has been finished and the packing of starch granules was underway.

3 | DISCUSSION

Tracing the Cd transportation with radioisotope ^{109}Cd can provide evidence of the transport characteristics of Cd in plants. To obtain the real picture of Cd behavior, it is important to consider carefully how to administrate ^{109}Cd to plant. In this study, rice plants were grown with full-nutrient solution added with $.1\ \mu\text{M}$ Cd under the controlled condition, and the dynamics of Cd absorbed from their roots at various time points after the start of the flowering were traced by using ^{109}Cd . So, we should discuss whether the ^{109}Cd absorbed from the root at the flowering stage represents the behavior of Cd in grains since 60% of the Cd in the mature grain has been estimated to be remobilized from that accumulated by the plant before flowering and the remainder came from root uptake after flowering (Rodda et al., 2011). In this regard, it should be noted that there is no report so far that shows Cd which is remobilized after flowering and Cd which is absorbed by the roots after flowering have different characteristics in terms of the transport in the vascular tissue in the ear. Indeed, the ^{109}Cd distribution in the double circle manner is consistent with the previous report finding the region with the higher Cd concentration surrounding the inner endosperm in the mature rice cultivated in the Cd-contaminated soil (Wei et al., 2017). Therefore, the pictures of ^{109}Cd distribution in the grain obtained in this study can be thought to represent the basic characteristics of Cd transport and accumulation in the rice grain during maturation. In field cultivation, the supply of Cd will not be constant throughout the grain development season. If there is a period when Cd supply is high, the distribution of Cd in the final harvested brown rice could have a distribution pattern being modified to emphasize the tissue where Cd accumulates during that period. In reality, paddy water management, which has a major impact on soil Cd availability, will play a critical role in shaping the Cd distribution pattern in grains (Gu et al., 2020). Regarding the perspective of quantity, another point to note is that, due to the relatively short period of ^{109}Cd labeling in this study, it is possible that the ratio of ^{109}Cd to stable Cd did not reach the steady state. Therefore, the ratio would not be identical among the grains, even in the same seedling. This means that the quantitative comparison of the total amount of Cd among grains based on the ^{109}Cd signal intensity will not be made accurately. We should focus on the distribution pattern of ^{109}Cd , as well as other radiotracers, in each autoradiograph presented in this study.

The autoradiographs of ^{109}Cd suggested that Cd distributes uniformly in the expanding rice endosperm from 3 DAF to 7 DAF, and then preferentially accumulated around the center of the endosperm from 8 DAF to 10 DAF to appear the inner circle of the double circle, and thereafter, deposited at the outer part of the endosperm. We

could not explain the mechanism underlying this Cd behavior simply based on our current knowledge. However, by making several assumptions, the Cd accumulation model can be suggested as illustrated in Figure 5. In this model, Cd is assumed to preferentially bind to glutelin in the protein body II (PB-II). Glutelin, which consists of 2 subunits, is the major seed storage protein in rice endosperm, accounting for about 80% of total seed protein (Yamagata et al., 1982). Several previous studies showed that the extraction behavior of Cd, compared to other metals, was similar to glutelin during chemical separation (Kitagishi et al., 1976; Moritsugu, 1964; Suzuki et al., 1997). It should be also noted the two observations that Cd-glutelin complex is significantly stabilized in the alkalinized solution with a pH higher than 6 (Kobashi et al., 1978), and that glutelin is formed via Golgi apparatus where the pH can be between 6.3 and 7.0 (Zhu et al., 2019). The time when accumulation of glutelin begins was shown to be 8 DAF (Takahashi et al., 2019), which is the same as the time when the inner circle of Cd appeared (Figure 2). In addition, one of the glutelin genes, *GluD-1*, was supposed to start expressing in the inner endosperm by 7 DAF, and then throughout the endosperm by 15 DAF (Kawakatsu et al., 2008). Development of starch granules is also rapidly progressing from 7 DAF (which is almost identical to 7 DAF in this study) from the inner part of the endosperm (Wu et al., 2016). We also hypothesized about the transport pathway of water to be loaded from the dorsal vascular bundle, pathing through the center of the endosperm, and directed to the embryo tissue in the end. The entrance of the water, as well as nutrient molecules, from the dorsal vascular bundle has been suggested based on morphological and experimental observations (Wu et al., 2016). Nutrients reached to the central endosperm can be further loaded to the embryo through the apoplasm surrounding the embryo tissues (Wu et al., 2016), which we hypothesized was also occurring for water. The water flow between endosperm and embryo, although the direction of flow was not elucidated, was indicated by the nuclear magnetic resonance (MR) imaging experiment (Horigane et al., 2001). Then, in our Cd accumulation model, Cd moves into the endosperm from the dorsal vascular bundles along with the water flow, probably like carbohydrates do, and spreads uniformly before 7 DAF (Figure 5). The chemical form of Cd when it enters brown rice may be in ionic form, but it is more likely to exist as Cd-bound 13 kDa complex (Kato et al., 2010). At 8 DAF, starch granules start to mature at the center of the endosperm, and protein bodies may start to be produced in the inner endosperm. Then, Cd moving along the water flow can be bound to glutelin in the protein body II (PB-II), gradually forming the inner circle until 10 DAF (Figure 5). After 11 DAF, the area where PB-II is produced is gradually expanded to the peripheral of the endosperm, resulting in the deposition of Cd in this area. Nevertheless, given that ^{109}Cd did not penetrate to the center part of the endosperm after 11 DAF was also true for ^{14}C -sucrose (Figure 4a), accumulation of Cd in the outer part of the endosperm may occur due to the decreased solute flow apart from binding to glutelin. After all, the inner circle of the Cd accumulation will remain apparent until maturation, as the amount of Cd deposition in the outer endosperm can be lower than that around the center part of the endosperm. Here, the additional

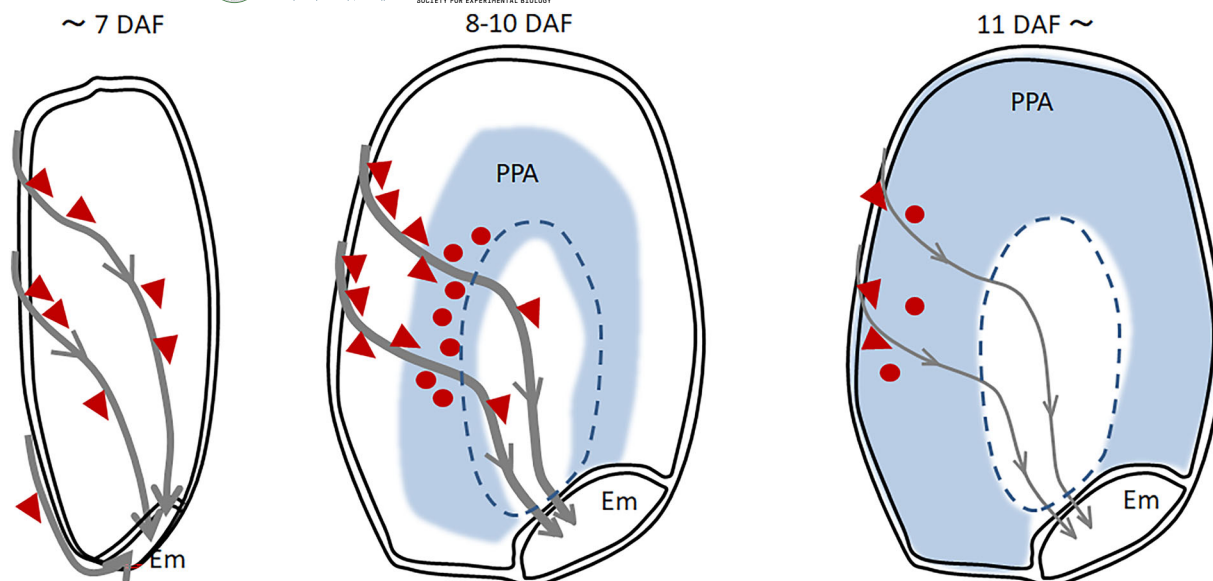


FIGURE 5 Schematic illustration representing a potential mechanism of Cd transport and deposition in the rice endosperm. By 7 DAF, as water and carbohydrates flow in, Cd also flows in and is distributed throughout the endosperm in the enlargement process. At the center of the endosperm, starch granules start to mature at 8 DAF, and then the protein body II (PB-II) starts to be synthesized at around the center of the endosperm. Water keeps flowing to the center of the endosperm, while Cd binds the glutelin in the PB-II and deposits before reaching the center of the endosperm. After 11 DAF, protein body production area (PPA) expands to the outer part of the endosperm. The amount of water and Cd flow in the endosperm decreases. In practice, water and cadmium inflows occur from all directions, but the figure shows only the inflow from the upper left as an example. The arrows indicate the flow of water, and their thickness indicates the volume of water. Triangles indicate Cd moving along the water flow, and circles indicate Cd binding to glutelin in PB-II and depositing there. The center of the endosperm where starch granules are dominated is enclosed by the dashed line. Em, embryo.

assumption needs to be made that the amount of Cd transported into the grain was decreased after 11 DAF. The actual amount of Cd accumulated in the endosperm during grain maturation in this study can not be quantitatively evaluated by the reason mentioned above. However, previous reports showed that the amount of Cd accumulated in a growing rice grain within 1 day peaked at around 9 DAF (Ren et al., 2023), and half of Cd in rice grains was loaded within 10 days after flowering (Rodda et al., 2011). The reduction of water flow into the endosperm after 10 DAF can be also suggested based on the MR images (Horigane et al., 2001).

For Zn dynamics, in contrast to Cd, deposition at the center part of the endosperm was found after 9 DAF without forming the inner circle-like distribution (Figure 1). This difference may be caused by differences in the binding properties to glutelin. For instance, Cd behaved almost identically to glutelin during chemical extraction, indicating a higher binding affinity to glutelin, while Zn was found both in the glutelin and non-protein fraction extracted by water (Kitagishi et al., 1976). It should be also noted that the concentration of Zn is, in fact, significantly higher than Cd in the starchy endosperm at the maturing stage. In the milled rice samples, concentrations of Zn and Cd were shown to be 18–20 mg kg⁻¹ and .022–.026 mg kg⁻¹, respectively (Tagami & Uchida, 2016). Therefore, it is reasonable to assume that Zn, which is present in high concentrations, binds nonspecifically to several compounds, including glutelin. Finally, before the grain matured completely, Zn in the center of the endosperm was thought to be loaded to the embryo along with the water flow. Thus, Zn

distributed almost uniformly in the mature rice endosperm and highly accumulated in the embryo, which is consistent with the elemental distribution maps visualized by synchrotron X-ray fluorescence microscopy (Gu et al., 2020; Johnson et al., 2011; Oli et al., 2016; Ren et al., 2023).

The signal of ¹⁰⁹Cd in the outer circle of the double circle at 11 DAF was shown to be emitted from the cross cells, the tube cells, and the seed coat tissue (Figure 3b). These cells are located between the vascular bundles and the endosperm, through which all solutes toward the endosperm will pass. During traveling through these cells, Cd might be sequestered in the vacuole and be accumulated. In fact, the inner integument cells in the seed coat are rich in vacuole and are suggested to be high in physiological activity, especially until 10 DAF (Matsuda et al., 1979). This result does not necessarily contradict previous literature that suggested Cd accumulation in the aleurone layer (Gu et al., 2020; Wei et al., 2017). Accumulation of Cd, although the amount could be small, was shown to continue in the outer endosperm after 11 DAF (Figure 2). Therefore, it is possible that at some time after 11 DAF, Cd is indeed deposited in the aleurone cells. It should be also noted that the cell layers in the outermost part of the brown rice including the cross cells, tube cells, and seed coat cells are degenerated and become thin after 18 DAF (Wu et al., 2016). It can be possible that the previous analysis could not distinguish between the layers of those degenerated cells and the adjacent aleurone layer in the mature brown rice due to the limited resolution. In any case, our result suggests that the cross cell, the tube cells, and the seed coat



cells take part in the regulation of Cd transport into the endosperm unless these tissues lose their physiological activity. In summary, the specific double circle distribution of Cd is assumed to have been formed under the influence of multiple physiological factors related to the grain development, including the amount of water and nutrients transported and their dynamics inside the brown rice, and changes in starch and protein biosynthesis and maturation over time.

4 | MATERIALS AND METHODS

4.1 | Rice plant cultivation

Rice seeds (*Oryza sativa* L. var. Nipponbare) were surface sterilized and then germinated in the tap water. The seedlings were cultivated hydroponically in the plant growth chamber (L/D = 10 h/14 h, 30 °C, 80% humidity). For cultivation, the half-strength Kimura B nutrient solution (Kobayashi et al., 2013) added with .1 μM CdCl₂ was used. The first ear appeared 46 days after germination.

4.2 | Administration of radionuclides and harvesting the grain samples

For administration of radionuclides, the root of the rice seedling was put in the nutrient solution added with the radionuclide. In addition to the dates and time of the start and end of radionuclide uptake, we recorded the date of the flowering for every single floret on the test plants using various colored markers. Flowers and seeds formed were used in the experiment solely according to the date of flowering, without regard to whether they were developed on the main stem or tillers, or their position in the panicle. To investigate the changes in the distribution of elements in the grain during the maturation process of brown rice, the radionuclides of Cd and Zn were kept being supplied to the roots from the ear emergence stage until the maturation stage, and the florets were sampled between 3 days after flowering (DAF) to 28 DAF. The radioactivity of the radionuclides used for this continuous administration was as follows: .65 kBq ml⁻¹ ¹⁰⁹CdCl₂ and 3.6 kBq ml⁻¹ ⁶⁵ZnCl₂. The series of experiments, from cultivation to sampling and visualization (described in the next and subsequent sections), was conducted twice, although the two experiments did not necessarily examine the same DAFs in all of them. Twenty-four hours of ¹⁰⁹Cd uptake was carried out with 17 kBq ml⁻¹ ¹⁰⁹CdCl₂. In selecting the test plants, we considered that in rice ear, the maximum number of flowers blooming per day reached 2 or 3 days after the first bloom. The seedlings with the maximum numbers of florets of 3 DAF, 6 DAF, 9 DAF, 12 DAF, or 15 DAF were transferred to a hydroponic solution containing ¹⁰⁹Cd and cultivated for 24 hours, after which they were returned to a regular hydroponic solution. The targeted florets were harvested 1, 4, and 7 days after the end of ¹⁰⁹Cd uptake as well as at 26 DAF. It should be noted that for each DAF at the start of the ¹⁰⁹Cd addition, two plants were prepared for the treatment. However, the seeds sampled from these two plants were not distinguished

and were used in subsequent experiments without distinction. Phloem flow into the rice grain was monitored by tracing ¹⁴C-sucrose administered by the foliar application. The small cotton wool absorbent with ¹⁴C-sucrose solution (2 MBq ml⁻¹ in pure water) was attached on the flag leaf blade for 24 hours. After labeling, the leaf surface was wiped and cleaned with wet cotton wool. A precise comparison between ¹⁰⁹Cd and ¹⁴C-sucrose was made by simultaneous administration of ¹⁰⁹Cd from roots and ¹⁴C-sucrose from the flag leaf for 24 hours at 9 DAF or 15 DAF. Three or four brown rice samples of each of the same treatment were collected and immediately placed in the embedding material (SECM, SECTION-LAB Co. Ltd.) and freeze-embedded with liquid nitrogen. The root samples were also embedded at the corner of the sample blocks aiming to use them as the positioning markers in the imaging process. The embedded sample blocks were stored in the deep freezer until sectioning.

4.3 | Preparation of fresh-frozen sections

Frozen sections were prepared by the film method using a cryotome (CM1850, Leica) set to -25°C as described previously (Kobayashi et al., 2013). Cryofilm TypeIC (SECTION-LAB Co. Ltd.) was used as the adhesive film for complete retention of the thin section. The thickness of the transverse section was 5 μm, and one section was taken sequentially every 100 μm. The number of sections obtained from one grain sample varied between 48 and 54, depending on the grain size.

4.4 | Autoradiography and 3D image construction

The sections with the adhesive film were placed on the sticky sponge sheet, wrapped with 1.2 μm thick polyphenylene sulfide film, and contacted to the imaging plate (IP BAS-TR, GE Healthcare) for 5 days under -80°C. After exposure, the imaging plate was scanned with the FLA-5000 image scanner (Fujifilm) with a resolution of 10 μm/pixel. The autoradiogram data were loaded in the ImageJ software using the ISAC Manager plugin to construct the image with original photo-stimulated luminescence (PSL) value. Individual section images were cut from multiple sequential images to create a single superimposed image of all consecutive sections (this is called “stack” in ImageJ). The position and angle of each section image were adjusted using the StackReg plugin (Thevenaz et al., 1998), and finally, three-dimensional image data were obtained by entering settings where 1 pixel in the XY direction was 10 μm and the spacing between sections was 100 μm.

4.5 | Autoradiography with discrimination between ¹⁴C and ¹⁰⁹Cd

The radiation emitted by ¹⁴C and ¹⁰⁹Cd from the grain administered both ¹⁴C-sucrose and ¹⁰⁹Cd was detected using the imaging plate

(IP BAS-TR, GE Healthcare). Discrimination between the two radionuclides was achieved based on differences in the transmittance of the two radiations. At first, the section samples were contacted to the imaging plate to detect both ^{14}C and ^{109}Cd . Then, the second exposure was made with the silver foil of 20 μm thickness inserted between the section samples and the imaging plate, which enabled to shield the radiation emitted by ^{14}C and leave only the ^{109}Cd signal (Figure S2). The ^{14}C plus ^{109}Cd signal image and ^{109}Cd signal image were overlaid using ImageJ software. After smoothing by Gaussian Blur processing, the Image Calculator plugin was used to acquire the subtracted signal as a ^{14}C distribution image.

4.6 | Microautoradiographic methods for high-resolution imaging

Distribution of ^{109}Cd was analyzed at the cellular level by means of the microautoradiography (MAR) based on the daguerreotype. To get an overview of ^{109}Cd distribution in the whole brown rice, “separated MAR” method, in which the section sample and the silver particles produced in the nuclear emulsion were observed separately (Hirose et al., 2014), was applied. Briefly, the frozen section sample on the adhesive film and the nuclear emulsion (Ilford Nuclear Emulsion Type K5; Harman Technology Ltd.) coated on the glass slide were placed on top of each other with the 1.2 μm thick polyphenylene sulfide film in between under dark and -25°C condition. After exposure in the -80°C ultra-low temperature freezer, the section sample, the polyphenylene sulfide film, and the nuclear emulsion film were separated. The nuclear emulsion film was soaked in quarter-strength Kodak D-19 developer (Kodak Ltd.) to develop the silver grains and observed with the microscope (BX-60, Olympus). The section sample was stained with hematoxylin–eosin and then observed with the microscope. The tissue images and radiographs were constructed and superimposed using ImageJ (Abramoff et al., 2004) and GIMP software (<http://www.gimp.org>). To achieve precise alignment of the silver particles and the rice tissue at the cellular level, “non-separated MAR” method was implemented. In this method, the cover glass was coated with the nuclear emulsion, and the section samples with the adhesive film were directly placed on it to exposure. Then, the cover glass coated with the nuclear emulsion with the section sample stuck on it was soaked with hexane to remove the adhesive film under dark and -25°C condition, followed by the graded series of ethanol to hydrate the nuclear emulsion in the dark room. After that, the development process was proceeded without separating the section samples. For microscopic observation, the sections were placed in contact with a glass slide, so that the cover glass came to the top. By changing the depth of focus, the brown rice tissue and the silver particles formed on it were observed separately. This non-separated MAR method is a technique with a very low success rate because the sections are often detached during the process of immersion in multiple solutions, but it has an outstanding advantage with respect to alignment of radiographs and tissue images.

4.7 | Observation of endosperm transparency

The rice grains of 9, 10, 11, and 13 DAF were sampled and embedded in the embedding material (SCEM, SECTION-LAB Co. Ltd.) under -25°C . The sample block was cut to near the center of the grain using a cryotome (CM1850, Leica). Then, the block was removed from the sample folder, turned upside down, and set back on the sample folder. Cutting was restarted and then stopped when the remaining sample was 1 mm thick. The 1 mm thick grain section was examined using an optical scanner.

AUTHOR CONTRIBUTIONS

Atsushi Hirose: Conceptualization and investigation. **Keitaro Tanoi:** Project administration. **Tomoko M. Nakanishi:** Supervision and funding acquisition. **Natsuko I. Kobayashi:** Conceptualization and writing—original draft; funding acquisition.

ACKNOWLEDGMENTS


The authors are grateful to all members of the management office of the radioisotope facility for their great effort in constructing the working environment for our research.

CONFLICT OF INTEREST STATEMENT

No conflict of interest was declared.

ORCID

Atsushi Hirose  <https://orcid.org/0000-0003-0390-223X>

Natsuko I. Kobayashi  <https://orcid.org/0000-0002-1279-7083>

REFERENCES

- Abramoff, M. D., Magelhaes, P. J., & Ram, S. J. (2004). Image processing with ImageJ. *Biophotonics International*, 11, 36–42.
- Abumaizar, R. J., & Smith, E. H. (1999). Heavy metal contaminants removal by soil washing. *Journal of Hazardous Materials*, 70(1–2), 71–86. [https://doi.org/10.1016/s0304-3894\(99\)00149-1](https://doi.org/10.1016/s0304-3894(99)00149-1)
- Arao, T., Kawasaki, A., Baba, K., Mori, S., & Matsumoto, S. (2009). Effects of water management on cadmium and arsenic accumulation and dimethylarsinic acid concentrations in Japanese rice. *Environmental Science & Technology*, 43, 9361–9367. <https://doi.org/10.1021/es9022738>
- Carrijo, D. R., LaHue, G. T., Parikh, S. J., Chaney, R. L., & Linquist, B. A. (2022). Mitigating the accumulation of arsenic and cadmium in rice grain: A quantitative review of the role of water management. *The Science of the Total Environment*, 839, 156245. <https://doi.org/10.1016/j.scitotenv.2022.156245>
- FAO/WHO. (2011a). *Joint FAO/WHO Expert Committee on Food Additives. Meeting (72nd: 2010: Rome, Italy)*. World Health Organization.
- FAO/WHO. (2011b). *World Health Organization, Food and Agriculture Organization of the United Nations & Joint FAO/WHO Expert Committee on Food Additives. Meeting (73rd: 2010: Geneva, Switzerland)*. World Health Organization. <https://apps.who.int/iris/handle/10665/44515>
- Gu, Y., Wang, P., Zhang, S., Dai, J., Chen, H. P., Lombi, E., Howard, D. L., van der Ent, A., Zhao, F. J., & Kopittke, P. M. (2020). Chemical speciation and distribution of cadmium in rice grain and implications for bioavailability to humans. *Environmental Science & Technology*, 54, 12072–12080. <https://doi.org/10.1021/acs.est.0c03001>
- Hachinohe, M., Okunishi, T., Hagiwara, S., Todoriki, S., Kawamoto, S., & Hamamatsu, S. (2015). Distribution of radioactive cesium (^{134}Cs)



- plus 137Cs) in rice fractions during polishing and cooking. *Journal of Food Protection*, 78, 561–566. <https://doi.org/10.4315/0362-028x.jfp-14-275>
- Hirose, A., Kobayashi, N. I., Tanoi, K., & Nakanishi, T. M. (2014). A micro-radiographic method for fresh-frozen sections to reveal the distribution of radionuclides at the cellular level in plants. *Plant and Cell Physiology*, 55, 1194–1202. <https://doi.org/10.1093/pcp/pcu056>
- Horigane, A. K., Engelaar, W. M. H. G., Maruyama, S., Yoshida, M., Okubo, A., & Nagata, T. (2001). Visualisation of moisture distribution during development of rice caryopses (*Oryza sativa* L.) by nuclear magnetic resonance microimaging. *Journal of Cereal Science*, 33(1), 105–114. <https://doi.org/10.1006/jcrs.2000.0348>
- Johnson, A. A. T., Kyriacou, B., Callahan, D. L., Carruthers, L., Stangoulis, J., Lombi, E., & Tester, M. (2011). Constitutive overexpression of the OsNAS gene family reveals single-gene strategies for effective iron and zinc-biofortification of rice endosperm. *PLoS ONE*, 6, e24476. <https://doi.org/10.1371/journal.pone.0024476>
- Kato, M., Ishikawa, S., Inagaki, K., Chiba, K., Hayashi, H., Yanagisawa, S., & Yoneyama, T. (2010). Possible chemical forms of cadmium and varietal differences in cadmium concentrations in the phloem sap of rice plants (*Oryza sativa* L.). *Soil Science and Plant Nutrition*, 56, 839–847. <https://doi.org/10.1111/j.1747-0765.2010.00514.x>
- Kawakatsu, T., Yamamoto, M. P., Hirose, S., Yano, M., & Takaiwa, F. (2008). Characterization of a new rice glutelin gene GluD-1 expressed in the starchy endosperm. *Journal of Experimental Botany*, 59, 4233–4245. <https://doi.org/10.1093/jxb/ern265>
- Khaokaew, S., Chaney, R. L., Landrot, G., Ginder-Vogel, M., & Sparks, D. L. (2011). Speciation and release kinetics of cadmium in an alkaline paddy soil under various flooding periods and draining conditions. *Environmental Science and Technology*, 45, 4249–4255. <https://doi.org/10.1021/es103971y>
- Kitagishi, K., Ohashi, M., Tokai, Y., & Umehayashi, M. (1976). Distribution and localization of heavy metals within rice grain, produced on paddy fields contaminated with cadmium, and chemical forms of cadmium in rice endosperms. *Report of the Environmental Sciences, Mie University*, 1, 129–141.
- Kobashi, K., Nakai, N., Hase, J., Miyahara, T., Kozuka, H., & Fujii, M. (1978). Chemical forms of cadmium in cadmium-polluted rice. I. Binding properties of glutelin-cadmium complex. *Eisei Kagaku*, 24, 314–321. <https://doi.org/10.1248/jhs1956.24.314>
- Kobayashi, N. I., Saito, T., Iwata, N., Ohmae, Y., Iwata, R., Tanoi, K., & Nakanishi, T. M. (2013). Leaf senescence in rice due to magnesium deficiency mediated defect in transpiration rate before sugar accumulation and chlorosis. *Physiologia Plantarum*, 148, 490–501. <https://doi.org/10.1111/ppl.12003>
- de Livera, J., McLaughlin, M. J., Hettiarachchi, G. M., Kirby, J. K., & Beak, D. G. (2011). Cadmium solubility in paddy soils: Effects of soil oxidation, metal sulfides and competitive ions. *Science of the Total Environment*, 409, 1489–1497. <https://doi.org/10.1016/j.scitotenv.2010.12.028>
- Makino, T., Kamiya, T., & Takano, H. (2011). Cadmium contents of soil and rice grains after bench-scale washing with biodegradable chelating agents. *Pedologist*, 54, 194–201. https://doi.org/10.18920/pedologist.54.3_194
- Makino, T., Kamiya, T., Takano, H., Itou, T., Sekiya, N., Sasaki, K., Maejima, Y., & Sugahara, K. (2007). Remediation of cadmium-contaminated paddy soils by washing with calcium chloride: Verification of on-site washing. *Environmental Pollution*, 147, 112–119. <https://doi.org/10.1016/j.envpol.2006.08.037>
- Matsuda, T., Kawahara, H., & Chonan, N. (1979). Histo-cytological researches on translocation and ripening in rice ovary. I. Histological changes and transfer pathways in the developing ovary. *Japanese Journal of Crop Science*, 48, 155–162. <https://doi.org/10.1626/jcs.48.155>
- Moritugu, M. (1964). A study on combination of glutelin with cadmium in rice grain. *Berichte des Ohara Instuts fur landwirtschaftliche Biologie*, 12, 251–260.
- Naito, S., Matsumoto, E., Shindoh, K., & Nishimura, T. (2015). Effects of polishing, cooking, and storing on total arsenic and arsenic species concentrations in rice cultivated in Japan. *Food Chemistry*, 168, 294–301. <https://doi.org/10.1016/j.foodchem.2014.07.060>
- Nakashima, S. (1979). Counter plants of paddy soils contaminated by cadmium and other heavy metals in Tsushima Island. *Bull Nagasaki Agr Fores Exp Strn*, 7, 337–385.
- Okuda, M., Hashiguchi, T., Joyo, M., Tsukamoto, K., Endo, M., Matsumaru, K., Goto-Yamamoto, N., Yamaoka, H., Suzuki, K., & Shimoi, H. (2013). The transfer of radioactive cesium and potassium from rice to sake. *Journal of Bioscience and Bioengineering*, 116, 340–346. <https://doi.org/10.1016/j.jbiosc.2013.03.001>
- Oli, P., Ward, R., Adhikari, B., Mawson, A. J., Adhikari, R., Wess, T., Pallas, L., Spiers, K., Paterson, D., & Torley, P. (2016). Synchrotron X-ray fluorescence microscopy study of the diffusion of iron, manganese, potassium and zinc in parboiled rice kernels. *Food Science and Technology*, 71, 138–148. <https://doi.org/10.1016/j.lwt.2016.03.034>
- Onozuka, H., Ebato, K., Amemiya, T., Mizuishi, K., Ono, Y., Fujii, T., & Onishi, K. (2000). The comparison of cadmium, copper and arsenic concentrations between unpolished and polished rice. *Tokyo-toritusu Eisei Kenkyusho Kenkyu Nenpo*, 51, 150–154. (in Japanese)
- Pedron, T., Segura, F. R., Paniz, F. P., de Moura, S. F., dos Santos, M. C., de Magalhães Júnior, A. M., & Batista, B. L. (2019). Mitigation of arsenic in rice grains by polishing and washing: Evidencing the benefit and the cost. *Journal of Cereal Science*, 87, 52–58. <https://doi.org/10.1016/j.jcs.2019.03.003>
- Ren, Z. W., Kopittke, P. M., Zhao, F. J., & Wang, P. (2023). Nutrient accumulation and transcriptome patterns during grain development in rice. *Journal of Experimental Botany*, 74, 909–930. <https://doi.org/10.1093/jxb/erac426>
- Rodda, M. S., Li, G., & Reid, R. J. (2011). The timing of grain Cd accumulation in rice plants: the relative importance of remobilisation within the plant and root Cd uptake post-flowering. *Plant and Soil*, 347, 105–114. <https://doi.org/10.1007/s11104-011-0829-4>
- Shindoh, K., & Yasui, A. (2003). Changes in cadmium concentration in rice during cooking. *Food Science and Technology Research*, 9, 193–196. <https://doi.org/10.3136/fstr.9.193>
- Suzuki, K. T., Sasakura, C., & Ohmichi, M. (1997). Binding of endogenous and exogenous cadmium to glutelin in rice grains as studied by HPLC/ICP-MS with use of a stable isotope. *Journal of Trace Elements in Medicine and Biology*, 11, 71–76. [https://doi.org/10.1016/S0946-672X\(97\)80029-6](https://doi.org/10.1016/S0946-672X(97)80029-6)
- Tagami, K., & Uchida, S. (2012). Radiocaesium food processing retention factors for rice with decreasing yield rates due to polishing and washing, and the radiocaesium distribution in rice bran. *Radioisotopes*, 61, 223–229. <https://doi.org/10.3769/radioisotopes.61.223>
- Tagami, K., & Uchida, S. (2016). Distributions of inorganic elements in brown rice determined by ICP-OES and ICP-MS, and analysis of their concentration changes by washing. *Bunseki Kagaku*, 65, 511–517. <https://doi.org/10.2116/bunsekikagaku.65.511>
- Takahashi, K., Kohno, H., Kanabayashi, T., & Okuda, M. (2019). Glutelin subtype-dependent protein localization in rice grain evidenced by immunodetection analyses. *Plant Molecular Biology*, 100, 231–246. <https://doi.org/10.1007/s11103-019-00855-5>
- Takijima, Y., Katsumi, F., & Koizumi, S. (1973). Cadmium contamination of soils and rice plants caused by zinc mining. V. Removal of soil cadmium by an HCl-leaching method for the control of high Cd rice. *Soil science and plant nutrition (Tokyo)*, 19, 245–254. <https://doi.org/10.1080/00380768.1973.10432594>
- Thevenaz, P., Ruttimann, U. E., & Unser, M. (1998). A pyramid approach to subpixel registration based on intensity. *IEEE Transactions on Image Processing*, 7, 27–41. <https://doi.org/10.1109/83.650848>

- Wei, S., Guo, B., Feng, L., Jiang, T., Li, M., & Wei, Y. (2017). Cadmium distribution and characteristics of cadmium-binding proteins in rice (*Oryza sativa* L.) kernel. *Food Science and Technology Research*, 23, 661–668. <https://doi.org/10.3136/fstr.23.661>
- Wu, X., Liu, J., Li, D., & Liu, C. (2016). Rice caryopsis development II: Dynamic changes in the endosperm. *Journal of Integrative Plant Biology*, 58, 786–798. <https://doi.org/10.1111/jipb.12488>
- Yamagata, H., Sugimoto, T., Tanaka, K., & Kasai, Z. (1982). Biosynthesis of storage proteins in developing rice seeds. *Plant Physiology*, 70, 1094–1100. <https://doi.org/10.1104/pp.70.4.1094>
- Yoshida, F. (2002). Itai-Itai disease and countermeasures against cadmium pollution by the Kamioka mine. In *The economics of waste and pollution management in Japan* (pp. 151–161). Springer Japan. https://doi.org/10.1007/978-4-431-67032-2_8
- Zhu, J., Ren, Y., Wang, Y., Liu, F., Teng, X., Zhang, Y., Duan, E., Wu, M., Zhong, M., Hao, Y., Zhu, X., Lei, J., Wang, Y., Yu, Y., Pan, T., Bao, Y., Wang, Y., & Wan, J. (2019). OsNHX5-mediated pH homeostasis is

required for post-Golgi trafficking of seed storage proteins in rice endosperm cells. *BMC Plant Biology*, 19, 295. <https://doi.org/10.1186/s12870-019-1911-y>

SUPPORTING INFORMATION

Additional supporting information can be found online in the Supporting Information section at the end of this article.

How to cite this article: Hirose, A., Tanoi, K., Nakanishi, T. M., & Kobayashi, N. I. (2024). Cadmium accumulation dynamics in the rice endosperm during grain filling revealed by autoradiography. *Plant Direct*, 8(1), e562. <https://doi.org/10.1002/pld3.562>